

A complete set of material properties of single domain $0.26\text{Pb}(\text{In}_{1/2}\text{Nb}_{1/2})\text{O}_3-0.46\text{Pb}(\text{Mg}_{1/3}\text{Nb}_{2/3})\text{O}_3-0.28\text{PbTiO}_3$ single crystals

Xiaozhou Liu,^{1,2} Shujun Zhang,¹ Jun Luo,³ Thomas R. Shrout,¹ and Wenwu Cao^{1,a)}

¹Materials Research Institute, The Pennsylvania State University, University park, Pennsylvania 16802, USA

²Key Laboratory of Modern Acoustics, Institute of Acoustics, Nanjing University, Nanjing 210093, People's Republic of China

³TRS technologies, Inc., 2820 East College Avenue, State College, Pennsylvania 16801, USA

(Received 2 November 2009; accepted 27 November 2009; published online 6 January 2010)

$\text{Pb}(\text{In}_{1/2}\text{Nb}_{1/2})\text{O}_3-\text{Pb}(\text{Mg}_{1/3}\text{Nb}_{2/3})\text{O}_3-\text{PbTiO}_3$ (PIN-PMN-PT) single crystals have been developed recently, which can increase the operating temperature by at least 20 °C compared to PMN-PT crystals. We have measured a complete set of material properties of single domain PIN-PMN-PT crystal, which is urgently needed in theoretical studies and electromechanical device designs using this crystal. Because the rotated values of $d_{33}^* = 1122$ pC/N and $k_{33}^* = 89\%$ along $[001]_c$ calculated using the single domain data obtained here are in good agreement with the $[001]_c$ poled multidomain PIN-PMN-PT crystals, one may conclude that the physical origin of the ultrahigh piezoelectric properties mainly come from orientation effect. © 2010 American Institute of Physics. [doi:10.1063/1.3275803]

The discovery of multidomain $\text{Pb}(\text{Mg}_{1/3}\text{Nb}_{2/3})\text{O}_3-\text{PbTiO}_3$ (PMN-PT) single crystals has triggered revolutionary changes in piezoelectric devices, particularly ultrabroad-band medical ultrasonic imaging transducers.¹ However, there are some limitations of PMN-PT ultrahigh piezoelectric crystals that prevent them from being used in certain applications. The most serious issue is the temperature stability because the rhombohedral to tetragonal phase transition temperature T_{RT} of PMN-PT system is only around 70 °C. In order to improve the temperature stability, people have added different dopants to push up T_{RT} . The ternary compound $\text{Pb}(\text{In}_{1/2}\text{Nb}_{1/2})\text{O}_3-\text{Pb}(\text{Mg}_{1/3}\text{Nb}_{2/3})\text{O}_3-\text{PbTiO}_3$ (PIN-PMN-PT) is the best found so far with the T_{RT} being increased by more than 20 °C without losing the superior piezoelectric properties.²⁻⁵

Up to date, all property characterizations of single crystals with ultrahigh piezoelectric properties have been limited to multidomain crystals^{2,6} due to two reasons: first, for practical applications, ultrahigh piezoelectric behavior only occurs in $[001]_c$ and $[011]_c$ polarized multidomain crystals, where the subscript “c” represents cubic coordinates; second, the single domain state is less stable than multidomain states, i.e., depoling often occurs in $[111]_c$ polarized single domain samples, which makes the full matrix property characterization extremely difficult. On the other hand, people are seeking better poling directions to achieve good properties using domain engineering method, but it is not possible to exhaust all orientations. It would be certainly more effective to have a complete set of single domain data to perform theoretical estimates of multidomain properties of different poling directions based on the principle of tensor rotation. In addition, such complete set single domain data is urgently needed for understanding the physical origin of such ultrahigh piezoelectric properties in these crystals.

In general, there are mainly two types of contributions to piezoelectric properties: intrinsic and extrinsic contributions. The extrinsic contribution from domain wall motions ac-

counts for more than 60% of the total effect in traditional piezoelectric ceramic $\text{Pb}(\text{Ti},\text{Zr})\text{O}_3$. On the other hand, theoretical analysis based on first principle's calculations had revealed that the rotation of polarization within the unit cell can play a critical role in the enhancement of piezoelectricity in domain engineered single crystals.⁷ In order to gain better understanding on the mechanism of such ultrahigh piezoelectric properties found in PIN-PMN-PT single crystals, single domain properties must be known.

Up to date, there is only one complete set of material constants available in the literature for single domain $0.67\text{Pb}(\text{Mg}_{1/3}\text{Nb}_{2/3})\text{O}_3-0.33\text{PbTiO}_3$ single crystal,⁸ which had facilitated theoretical analyses on the mechanism of ultrahigh piezoelectric effect in domain engineered PMN-PT single crystals. Based on the single domain data set, one could obtain rotated materials properties to quantify the orientation effect.^{9,10} It was confirmed that the ultrahigh piezoelectric constants were mainly from orientation effect due to the extremely high shear piezoelectric coefficient d_{15} of the single-domain state. Ahart *et al.*¹¹ reported the only other complete set of elastic and piezoelectric constants for single-domain rhombohedral $0.955\text{Pb}(\text{Zn}_{1/3}\text{Nb}_{2/3})\text{O}_3-0.045\text{PbTiO}_3$ (PZN-PT) using micro-Brillouin scattering technique, but their value of d_{33} is quite different from ultrasonic measure-

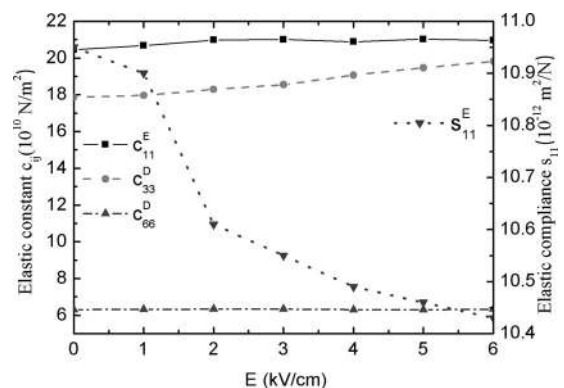


FIG. 1. Variation of elastic constants with bias field.

^{a)}Electronic mail: dzk@psu.edu.

TABLE I. Relationship between phase velocities and elastic constants for $3m$ symmetry and the measured values of phase velocities in $0.26\text{Pb}(\text{In}_{1/2}\text{Nb}_{1/2})\text{O}_3-0.46\text{Pb}(\text{Mg}_{1/3}\text{Nb}_{2/3})\text{O}_3-0.28\text{PbTiO}_3$ single-domain single crystals.

Phase velocities	$v_l^{[111]}$	$v_s^{[111]}$	$v_l^{[1\bar{1}0]}$	$v_{sll}^{[1\bar{1}0]}$	$v_{s\perp}^{[1\bar{1}0]}$	$v_l^{[11\bar{2}]}$	$v_{sll}^{[11\bar{2}]}$	$v_{s\perp}^{[11\bar{2}]}$
Related constants	c_{33}^D	c_{44}^E	c_{11}^E	c_1	c_2	c_3	c_{66}^E	c_4
Measured velocities (m/s)	4945	1610	5086	1457	3060	5017	2795	2804

ments. They have attributed the difference of rotated data with directly measured multidomain data to the strong frequency dispersion effect. Because conventional applications for these materials are usually less than 100 MHz, data obtained using ultrasonic and resonance techniques are more appropriate than from Brillouin scattering technique.

For PMN-PT and PZN-PT systems, the single domain state in the rhombohedral phase is rather unstable. Therefore, one cannot get the single domain data without using a bias field to assist the measurement.⁸ Similarly, the $[111]_c$ polarized single domain PIN-PMN-PT also suffers depoling effect although the domain stability is much better compared to PMN-PT and PZN-PT systems. The crystallographic symmetry of the single domain PMN-PIN-PT crystals is rhombohedral $3m$, there are total 12 independent material constants: 6 elastic, 4 piezoelectric, and 2 dielectric constants. Therefore, we need at least 12 independent measurements to fully determine them.

The PIN-PMN-PT crystal were grown by modified Bridgeman method and the samples measured in this work has the nominal composition of $0.26\text{Pb}(\text{In}_{1/2}\text{Nb}_{1/2})\text{O}_3-0.46\text{Pb}(\text{Mg}_{1/3}\text{Nb}_{2/3})\text{O}_3-0.28\text{PbTiO}_3$. Based on the dielectric measurements, we found that the Curie temperature T_c is about 167 °C while the rhombohedral to tetragonal phase transition temperature T_{RT} is about 123 °C, corresponding to the part A composition reported in Ref. 2. Crystal samples were oriented using the Laue x-ray machine with an accuracy of $\pm 0.5^\circ$. Each sample was cut and polished into a parallelepiped with three pairs of parallel surfaces along $[111]_c$, $[1\bar{1}0]_c$, and $[11\bar{2}]_c$, respectively. Gold electrodes were sputtered onto the $[111]$ and $[\bar{1}\bar{1}\bar{1}]$ faces of each sample

and an electric field of 15 kV/cm was used to pole these samples into single domain state above 100 °C, then slowly cooled down to room temperature. For the length and thickness extensional resonance measurements, the aspect ratios of samples exceeded 5:1 in order to yield pure resonance modes. To guarantee the single domain states, a 6 kV/cm bias field along the poling direction was applied during all measurements.

A 15 MHz longitudinal wave transducer (Ultran laboratories, Inc.) and a 20 MHz shear wave transducer (Panametrics) were used for the pulse-echo measurements. The electric pulses used to excite the transducer were generated by a Panametrics 200 MHz pulser/receiver, and the time of flight between echoes was measured using a Tektronix™ 460A digital oscilloscope. For the length and thickness resonance measurements, an HP 4194A impedance/gain phase analyzer was employed.

In order to check the effect of electric bias on the properties of PIN-PMN-PT, we first measured s_{11}^E as a function of the electric field using resonance method. As shown in Fig. 1, when a 6 kV/cm electric bias was applied, s_{11}^E changed from 10.95×10^{-12} to 10.43×10^{-12} N/m², c_{33}^D changed about 10% but c_{11}^E and c_{66}^E have almost no change. The reason is that the thickness of the sample for c_{33}^D measurement is thin (about 1 mm), which makes the single-domain structure unstable, while the thickness of the sample for measuring c_{11}^E and c_{66}^E are about 5 mm, for which the single-domain structure is rather stable.

We can get the elastic constants $c_{33}^D, c_{44}^E, c_{11}^E, c_{66}^E$, and the combinations of elastic constants c_1, c_2, c_3 , and c_4 form the phase velocity measurements,⁸ $k_{31}, k_{33}, k_t, k_{15}, s_{11}^E$, and s_{33}^D

TABLE II. Measured and derived material properties of PIN-PMN-PT single-domain single crystal poled in $[111]$ (Density: $\rho=8102$ kg/m³).

Elastic stiffness constants: c_{ij} (10^{10} N/m ²)															
c_{11}^E ^a	c_{12}^E	c_{13}^E	c_{14}^E	c_{33}^E	c_{44}^E ^a	c_{66}^E ^a	c_{11}^D	c_{12}^D	c_{13}^D	c_{14}^D	c_{33}^D ^a	c_{44}^D	c_{66}^D		
20.96	8.29	6.46	2.66	17.65	2.10	6.33	22.01	8.25	5.61	1.08	19.81	6.68	6.88		
Elastic compliance constants: s_{ij} (10^{-12} m ² /N)															
s_{11}^E ^a	s_{12}^E	s_{13}^E	s_{14}^E	s_{33}^E	s_{44}^E	s_{66}^E	s_{11}^D	s_{12}^D	s_{13}^D	s_{14}^D	s_{33}^D ^a	s_{44}^D	s_{66}^D		
10.43	-6.40	-1.49	-21.38	6.76	101.85	33.75	5.58	-1.87	-1.09	-1.21	5.88	15.36	14.91		
Piezoelectric coefficients: $e_{i\lambda}$ (C/m ²)															
e_{15}	e_{22}	e_{31}	e_{33}	d_{15}	d_{22}	d_{31}	d_{33}	g_{15}	g_{22}	g_{31}	g_{33}	h_{15}	h_{22}	h_{31}	h_{33}
18.78	6.48	-5.19	8.72	2190	511	-34	74	3.93	0.92	-0.55	1.20	24.39	8.41	-9.74	16.38
Dielectric constants: $\epsilon(\epsilon_0)$															
ϵ_{11}^S ^a	ϵ_{33}^S ^a	ϵ_{11}^T ^a	ϵ_{33}^T ^a	β_{11}^S	$\beta(10^{-4}/\epsilon_0)$				Electromechanical coupling factors $k_{i\lambda}$						
870	601	6286	702	11.49	β_{33}^S	β_{11}^T	β_{33}^T	k_{15} ^a	k_{31} ^a	k_{33} ^a	k_t ^a				
					16.63	15.91	14.24	0.92	0.13	0.36	0.33				

^aReference 12.

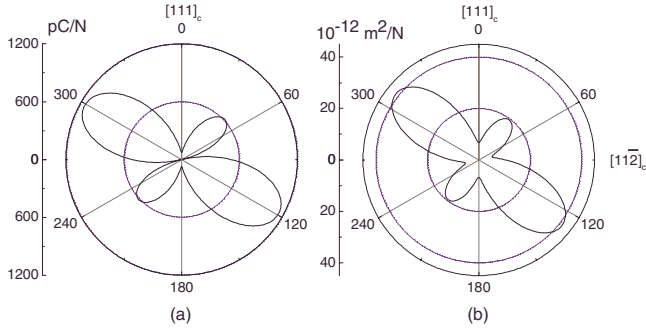


FIG. 2. (Color online) (a) Orientation dependence of piezoelectric constant d_{33}^* ; (b) Elastic compliance s_{33}^* of single domain $0.26\text{Pb}(\text{In}_{1/2}\text{Nb}_{1/2})\text{O}_3-0.46\text{Pb}(\text{Mg}_{1/3}\text{Nb}_{2/3})\text{O}_3-0.28\text{PbTiO}_3$ single crystal.

from the resonance technique. In addition, dielectric constants such as ϵ_{11}^T , ϵ_{11}^S , ϵ_{33}^T , and ϵ_{33}^S can be obtained directly from low and high frequency capacitance measurements. Over all, we have obtained 18 independent measurements for the 12 independent constants. The six extra measurements provided control checks to guarantee the self consistency of the full matrix data.

The measured phase velocities of longitudinal and shear waves along different crystallographic directions in the single-domain PIN-PMN-PT crystals are listed in Table I, where $v_l, v_{s\parallel}, v_{s\perp}$ denote longitudinal velocity and shear velocities with displacement parallel and perpendicular to the polarization direction, respectively. The measured and derived material properties of PIN-PMN-PT single-domain single crystal poled in $[111]_c$ are summarized in Table II. One can see that d_{15} (~ 2190 pC/N) in the single domain state is much larger than that in multidomain state (~ 119 pC/N).²

Based on the single-domain data of PIN-PMN-PT given in Table II, we have calculated the orientation dependence of piezoelectric constant d_{33}^* , elastic compliance s_{33}^* , dielectric constant ϵ_{33}^* , and electromechanical coupling factor k_{33}^* as shown in Figs. 2 and 3, respectively. The maximum values of d_{33}^* , k_{33}^* , ϵ_{33}^* , and s_{33}^* occur at 64.1° , 79.2° , 90° , and 52.3° , respectively, from the spontaneous polarization direction. In the $[001]_c$ direction, the calculated values are $d_{33}^* = 1122$ pC/N, $k_{33}^* = 89\%$, $\epsilon_{33}^* = 4360$, and $s_{33}^* = 41.00 \times 10^{-12}$ N/m², which agree well with the experimental results ($d_{33}^* = 1130$ pC/N, $k_{33}^* = 89\%$, $\epsilon_{33}^* = 4000$, and $s_{33}^* = 45.7 \times 10^{-12}$ N/m² for part A of PIN-PMN-PT single crystal boule reported in Ref. 2).

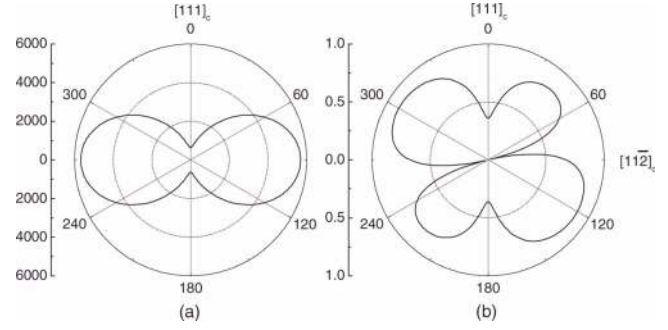


FIG. 3. (Color online) (a) Orientation dependence of dielectric constant ϵ_{33}^* ; (b) electromechanical coupling factor k_{33}^* of single domain $0.26\text{Pb}(\text{In}_{1/2}\text{Nb}_{1/2})\text{O}_3-0.46\text{Pb}(\text{Mg}_{1/3}\text{Nb}_{2/3})\text{O}_3-0.28\text{PbTiO}_3$ single crystal.

In summary, we have measured a complete set elastic, piezoelectric, and dielectric constants of single-domain $0.26\text{Pb}(\text{In}_{1/2}\text{Nb}_{1/2})\text{O}_3-0.46\text{Pb}(\text{Mg}_{1/3}\text{Nb}_{2/3})\text{O}_3-0.28\text{PbTiO}_3$ using a hybrid method. The piezoelectric properties of this crystal is similar to that of PMN-0.28PT, but the corresponding phase transition temperatures, T_{RT} and T_c , are more than 20°C higher. Through tensor rotation of the measured single domain data we found that the ultrahigh piezoelectric properties of $[001]_c$ poled PIN-PMN-PT are mainly from orientation effect.

This research was supported by the NIH under Grant No. P41-EB21820 and ONR under Grant Nos. N00014-09-01-0456 and N00014-07-C-0858.

¹Philips Vision 2007 new product release. Details of this PureWave transducer can be found in the following webpage: <http://www.medical.philips.com/main/products/ultrasound/technologies/purewave.wpd>.

²S. Zhang, J. Luo, W. Hackenberger, and T. R. Shrout, *J. Appl. Phys.* **104**, 064106 (2008).

³G. S. Xu, K. Chen, D. F. Yang, and J. B. Li, *Appl. Phys. Lett.* **90**, 032901 (2007).

⁴J. Tian, P. D. Han, X. L. Huang, and H. X. Pan, *Appl. Phys. Lett.* **91**, 222903 (2007).

⁵S. J. Zhang, J. Luo, W. Hackenberger, N. P. Sherlock, R. J. Meyer, Jr., and T. R. Shrout, *J. Appl. Phys.* **105**, 104506 (2009).

⁶X. Z. Liu, S. J. Zhang, J. Luo, T. R. Shrout, and W. Cao, *J. Appl. Phys.* **106**, 074112 (2009).

⁷H. Fu and R. E. Cohen, *Nature (London)* **403**, 281 (2000).

⁸R. Zhang, B. Jiang, and W. Cao, *Appl. Phys. Lett.* **82**, 787 (2003).

⁹R. Zhang, B. Jiang, and W. Cao, *Appl. Phys. Lett.* **82**, 3737 (2003).

¹⁰D. Damjanovic, M. Budimir, M. Davis, and N. Setter, *Appl. Phys. Lett.* **83**, 2490 (2003).

¹¹M. Ahart, A. Asthagiri, P. Dera, H.-K. Mao, R. E. Cohen, and R. J. Hemley, *Appl. Phys. Lett.* **88**, 042908 (2006).

¹²Directly measured properties is represented by "a" in Table II.